DeepWeeds: A Multiclass Weed Species Image Dataset for Deep Learning

Alex Olsen^{1,*}, Dmitry A. Konovalov², Bronson Philippa¹, Peter Ridd¹, Jake C. Wood¹, Jamie Johns¹, Wesley Banks¹, Benjamin Girgenti¹, Owen Kenny¹, James Whinney¹, Brendan Calvert¹, Mostafa Rahimi Azghadi¹, and Ronald D. White¹

ABSTRACT

Robotic weed control has seen increased research in the past decade with its potential for boosting productivity in agriculture. Majority of works focus on developing robotics for arable croplands, ignoring the significant weed management problems facing rangeland stock farmers. Perhaps the greatest obstacle to widespread uptake of robotic weed control is the robust detection of weed species in their natural environment. The unparalleled successes of deep learning make it an ideal candidate for recognising various weed species in the highly complex Australian rangeland environment. This work contributes the first large, public, multiclass image dataset of weed species from the Australian rangelands; allowing for the development of robust detection methods to make robotic weed control viable. The *DeepWeeds* dataset consists of 17,509 labelled images of eight nationally significant weed species native to eight locations across northern Australia. This paper also presents a baseline for classification performance on the dataset using the benchmark deep learning models, Inception-v3 and ResNet-50. These models achieved an average classification performance of 87.9% and 90.5%, respectively. This strong result bodes well for future field implementation of robotic weed control methods in the Australian rangelands.

Introduction

Robotic weed control promises a step-change in agricultural productivity^{1,2}. The primary benefits of autonomous weed control systems are in reducing the labour cost while also potentially reducing herbicide usage with more efficient selective application to weed targets. Improving the efficacy of weed control would have enormous economic impact. In Australia alone, it is estimated that farmers spend AUD\$1.5 billion each year on weed control activities and lose a further \$2.5 billion in impacted agricultural production³. Successful development of agricultural robotics is likely to reduce these losses and improve productivity.

Research in robotic weed control has focused on what many consider to be the four core technologies: detection, mapping, guidance and control⁴. Of these, detection remains a significant obstacle toward commercial development and industry acceptance of robotic weed control technology^{4,5}. Three primary methods of detection exist that focus on different representations of the light spectrum. Varied success has been achieved using image-based⁶⁻¹⁵, spectrum-based^{16,17} and spectral image-based^{18,19} methods to identify weeds from both ground and aerial photography. Spectrum and spectral image-based methods are most suitable for highly controlled, site-specific environments, such as arable croplands where spectrometers can be tailored to their environment for consistent acquisition and detection. However, the harsh and complex rangeland environment make spectral-based methods challenging to implement, while image-based methods benefit from cheaper and simpler image acquisition in varying light conditions, especially when deployed in a moving vehicle in real time²⁰. Thus for this work, we focus on image-based techniques for recognising weed species.

The automatic recognition of plants using computer vision algorithms is an important academic and practical challenge²¹. One way of solving this challenge is to identify plants from their leaf images^{7,9–15}. A variety of algorithms and methods have been developed to solve this problem²². Perhaps the most promising recent leaf-classification methods are based on deep learning models, such as Convolutional Neural Networks (CNN)^{7,13,14,23}; which now dominate many computer vision related fields. For example, the ImageNet Large Scale Visual Recognition Challenge (ILSVRC) has been dominated by CNN variants since 2012 when a CNN²⁴ won for the first time, and by a wide margin. This and other recent successes behoove the use of deep learning in the detection and identification of weed species.

¹College of Science and Engineering, James Cook University, Townsville, QLD, 4811, Australia

²College of Business, Law and Governance, James Cook University, Townsville, QLD, 4811, Australia

^{*}Correspondence and requests for materials should be addressed to alex.olsen@my.jcu.edu.au

The performance of every machine learning model, from simple linear regression to complex CNNs, is bound by the dataset it is learning. The literature boasts many weed and plant life image datasets ^{9,10,14,21}. The annual LifeCLEF plant identification challenge^{25–27} presented a 2015 dataset²⁵ composed of 113,205 images belonging to 41,794 observations of 1,000 species of trees, herbs and ferns. This sprawling dataset is quite unique, with most other works presenting site-specific datasets for their weeds of interest^{9,14,21}. These approaches all deliver high detection accuracy for their target datasets. However, most datasets capture their target plant life under perfect lab conditions^{9,14}. While the perfect lab conditions allow for strong theoretical classification results, deploying a detection model on a weed control robot requires an image dataset that photographs the plants under realistic environmental conditions. Figure 1 illustrates the comparative difficulty of detecting species in situ. 1a

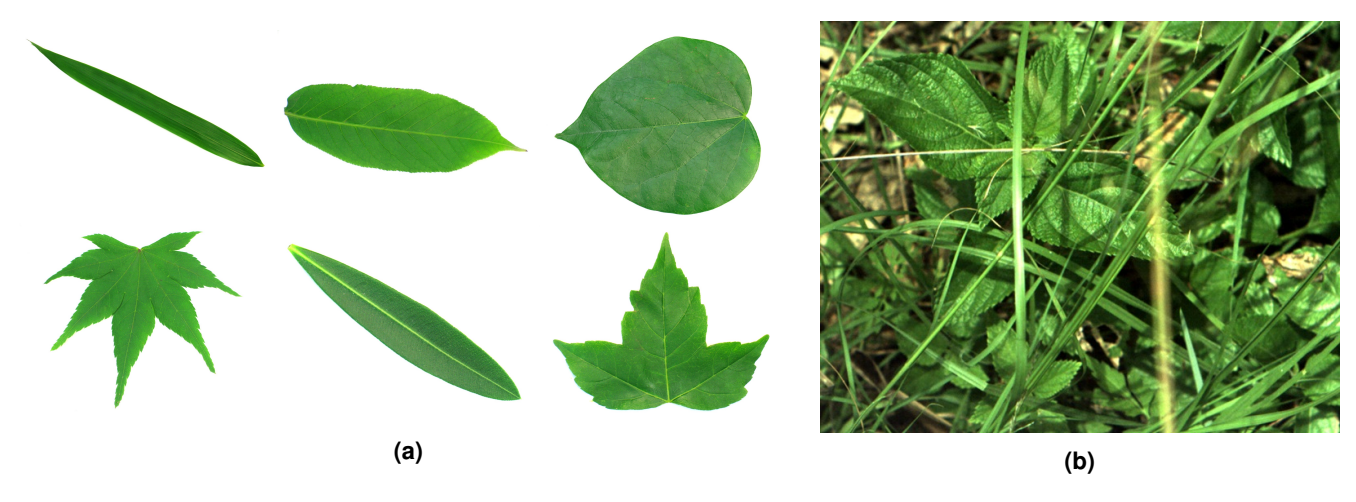


Figure 1. A comparison of the inherent difficulty associated with detecting weed species in the lab versus in the field. (a) Sample images from the Flavia leaf image dataset taken in a controlled lab environment from their leaf material. (b) A sample image of lantana from the *DeepWeeds* dataset, taken in situ capturing a realistic view of the entire plant.

The majority of current weed species detection methods also lean towards weed control in cropping applications^{7,28–30}, where detection using machine vision is simple because the land is often flat, vegetation homogeneous and the light conditions are controlled. Detection of weeds in rangeland environments, however, has been largely ignored. Rangeland environments pose unique challenges for weed management and detection because they are remote and extensive, with rough and uneven terrain, and complex target backgrounds. Furthermore, many different species of weeds and native plants may also be present in the same area, all at varying distances from the camera, each experiencing different levels of light and shade, with some weeds being entirely hidden. To allow the detection methods deployed in this environment any chance of success, site-specific and highly variable weed species image datasets are needed.

Liaison with land care groups and property owners across northern Australia led to the selection of eight target weed species for the the collection of a large weed species image dataset; (1) chinee apple (*Ziziphus mauritiana*), (2) lantana (*Lantana camara*), (3) parkinsonia (*Parkinsonia aculeata*), (4) parthenium (*Parthenium hysterophorus*), (5) prickly acacia (*Vachellia nilotica*), (6) rubber vine (*Cryptostegia grandiflora*), (7) siam weed (*Chromolaena odorata*) and (8) snakeweed (*Stachytarpheta spp.*). These species were selected because of their suitability for foliar herbicide spraying, and their notoriety for invasiveness and damaging impact to rural Australia. Five of the eight species have been targeted by the Australian Government as *Weeds of National Significance* in a bid to limit their potential spread and socio-economic impacts³¹.

In this study, we present the *DeepWeeds* dataset, containing 17,509 images of eight different weed species labelled by humans. The images were collected in situ from eight rangeland environments across northern Australia. Furthermore, we train a deep learning image classifier to identify the species that are present in each image. We anticipate that the dataset and our classification results will inspire further research into the detection of rangeland weeds under realistic conditions as would be experienced by an autonomous weed control robot.

Methods

Dataset Collection

The first goal of this work was the collection of a large labelled dataset to facilitate the detection and classification of a variety of weed species for robotic weed control. The emerging trend of deep learning for object detection necessitates its use for this task. As a result, careful consideration was taken for key factors to aid the learning process. These factors include: the optical system, scene variability, dataset size, weed targets, weed locations, negative samples, image metadata and labelling.

Oftentimes image processing frameworks fail in real world application because they are hamstrung by unforeseen errors during the first and most important step in the framework: image acquisition³². The images acquired must match the target application as closely as possible for real world success. Our goal is to use the collected dataset to train a ground-based weed control robot; therefore, we must tailor the dataset to match this application. Our envisioned ground-based weed control solution incorporates arrays of high-resolution cameras and fast acting solenoid sprayers; at the front and back of the robotic vehicle, respectively. Its goal is to perform pass-over foliar herbicide spot spraying of identified weed targets. So as not to limit the vehicle's maneuverability, no external shading or lighting is to be used for the optical system.

A data logging instrument was developed to ensure consistent image acquisition and to accelerate the image collection process. The *WeedLogger* instrument, pictured in Figure 2, consists of a Raspberry Pi, high resolution camera, machine vision lens and a GPS receiver. Its custom software and touchscreen interface allows for in-field labelling of geo-mapped images.

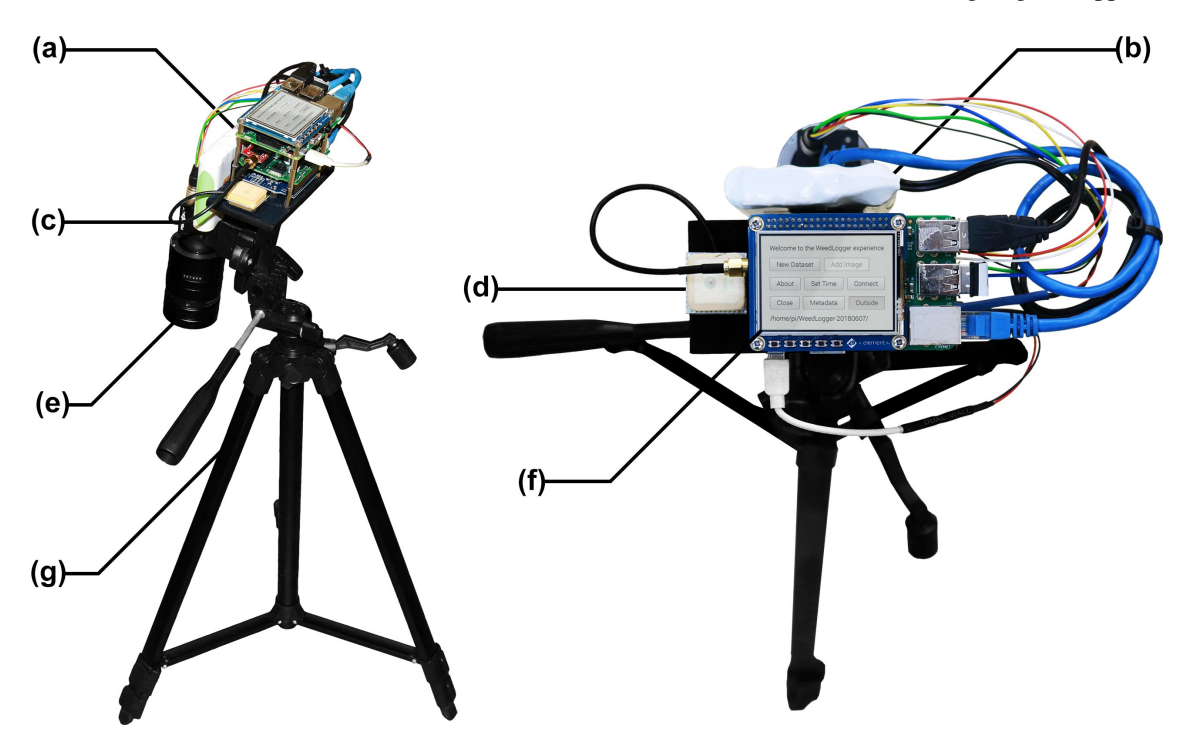


Figure 2. The *WeedLogger* field instrument was developed to facilitate the collection of time and GPS stamped images. The instrument consists of: (a) a Raspberry Pi 3, Arduino Uno and custom electronics shield, (b) a rechargeable lithium-ion battery pack, (c) a FLIR Blackfly 23S6C Gigabit Ethernet high-resolution colour camera, (d) a SkyTraq Venus638FLPx GPS receiver and V.Torch VTGPSIA-3 GPS antenna, (e) a Fujinon CF25HA machine vision lens, (f) a 4D Systems Raspberry Pi touchscreen display module and (g) an Inca i330G light-weight tripod.

Scene and target variability was a major design consideration for this dataset. When designing models or algorithms for learning features, our goal is to separate the factors of variation that explain the observed data³³. The *depth* of a deep learning model conceptually refers to said model's layer count and parameter complexity. Typically, the more confounding factors of variability in the dataset, the deeper and more complex the model required to achieve acceptable performance³³. To match the target real world application, we must abide several factors of variation, including: illumination, rotation, scale, focus, occlusion, dynamic backgrounds; as well as geographical and seasonal variation in plant life.

Illumination will vary throughout the day with changing sunlight and canopy cover creating highly dynamic range scenes with bright reflectance and dark shadows. Rotation and scale of the target weed species will vary as they are being photographed in situ with unknown size and orientation. The heights of photographed weed species are also variable. Therefore, the fixed focal region of the camera will cause some targets to be blurred and out of focus. Fortunately, motion blur is mitigated by operating with an extremely fast shutter speed. Because of this brief exposure time, the optical system has been chosen to have a large f/8 f-stop. Perhaps the most variability in the dataset is due to complex and dynamic target backgrounds. The locations subject to dense weed infestations are also inhabited by immeasurable counts of other native species. As we are unable to curate a dataset of all plant life, we must concede to labelling all other non-target plant life as *negative* samples; along with all non-target background imagery. Unfortunately, this creates a highly variable class in the dataset that will be difficult to consistently classify.

In addition to complex backgrounds, target foreground objects can be unexpectedly occluded from view by interfering objects; more often other neighbouring flora. This is yet another unavoidable factor of variation. Finally, the dataset must account for seasonal variation in our target weed species. This means that a single class of weed species will include photographs of the weed with and without flowers and fruits and in varying health condition; which can affect foliage colour, strength of features and other visible anomalies.

Two primary goals were established to achieve the required variability and generality of the dataset. First, collect at least 1,000 images of each target species. Second, attain a 50:50 split of positive to negative class images from each location. The first goal is a necessity when training high-complexity CNNs which require large labelled datasets. The second goal helps to prevent over-fitting of developed models to scene level image features by ensuring targets are detected from their native backgrounds. Finally, the dataset required expert analysis to label each image as to whether it contains a target weed species or not. The rigidity of this collection process will ensure that the accuracy and robustness of all learning models developed to classify from it, will be upheld when applied in the field. Figure 3 illustrates a sampling of images from each class in the dataset. From this, the complexity of the learning problem is apparent due to the inherent variation within classes of the dataset.

Deep Learning

The second goal of this study was to establish the baseline accuracy expected from modern deep learning CNNs; the state-of-the-art computer vision solution. An emphasis was given to off-the-shelf CNNs, which could be easily trained and deployed to facilitate wider use of the presented dataset. To that effect, the high-level neural network Application Programming Interface (API), Keras³⁴, was utilised; together with the machine learning framework, TensorFlow³⁵. Two popular CNN models were chosen for implementation based on their strong performance on highly variable datasets and their availability in the Keras and Tensorflow backend. The first model chosen, Inception-v3³⁶ (the third improvement upon the GoogLeNet³⁷ Inception architecture) was the winner of ILSVRC 2014³⁸; and the second, ResNet-50³⁹, was the winner of ILSVRC 2015³⁸. This annual competition sees participant models recognise 1,000 different ImageNet object classes from over 500,000 images. Other winners of the ILSVRC were considered at the time of writing. The comparable 2014 winner, VGGNets⁴⁰ was dismissed due to having 144 million training parameters compared to the more manageable 5 million parameters of Inception-v3. The 2016 ILSVRC winner, GBD-Net⁴¹, was not considered because it requires within-image per-pixel labels, which are not yet available for the *DeepWeeds* dataset. Furthermore, the 2017 competition winner, Squeeze-and-Excitation (SE) networks⁴² was not considered because the SE augmented models are not readily available in the Keras and Tensorflow backend.

The models considered henceforth, Inception-v3³⁶ and ResNet-50³⁹, are both available in Keras with pre-trained weights in the TensorFlow backend. The models were trained to recognise the 1,000 different ImageNet³⁸ object classes. Their original ImageNet-trained architectures were slightly modified to classify the nine *DeepWeeds* species classes. This was achieved by replacing their last densely-connected 1,000 neuron layer with a 9 neuron fully-connected layer. Specifically, let *b* denote the number of images per training batch, and *r* and *c* denote the number of pixel rows and columns, respectively. Each network then accepted a $b \times r \times c \times 3$ input matrix, where 3 was the number of image colour channels. After removing the 1,000 ImageNet classification layers, both network outputs had the $b \times r_{\alpha} \times c_{\alpha} \times f_{\alpha}$ shape, where α denotes the specific network, and f_{α} was the number of extracted features for each $r_{\alpha} \times c_{\alpha}$ spatial location. Identical to Inception-v3, the spatial average pooling layer was used to convert the fully-convolutional $b \times r_{\alpha} \times c_{\alpha} \times f_{\alpha}$ output to the $b \times f_{\alpha}$ shape, which was then densely connected to the final $b \times 9$ weed classification layer. With 32 images per batch and 224 × 224 × 3 sized input images, the deployed global average pooling was effectively identical to the 7 × 7 average pooling in the ResNet-50 model.

The nature of this classification task and the *DeepWeeds* dataset allows for multiple weed species to be present in each image. Therefore, a sigmoid activation function was used for each weed-specific neuron in the output layer. This allowed an output of probabilities for each class to identify the likelihood that an image belonged to each class. An image was classified as one of the target weeds if that class' sigmoid-activated neuron probability was the greatest amongst all others and its likelihood was greater than $1/9 = 11.\overline{1}\%$ (i.e. a random guess). The random guess threshold was implemented to overcome the immense variation in the negative *DeepWeeds* class, which causes its target probability to be less strongly weighted towards specific image features than the eight positive classes – whose images are more consistent.

All 17,509 labelled images from *DeepWeeds* were randomly partitioned into a 60%-20%-20% split of training, validation and testing subsets. The 60% random split constitutes the training subset, while 20% were used as the validation subset to monitor the training process and minimise overfitting. Each random split was controlled by a random seed such that the individual split could be reproduced as required. The remaining 20% of images were reserved for testing and were not used in any way during the training process. Before training, each model was loaded with the corresponding weights pre-trained on ImageNet. It was found that the ImageNet-trained models were more accurate and faster to train than randomly initialised CNNs when the models were re-purposed to recognise new object classes; this is often referred to as the *knowledge transfer*⁴³. The weights of the 9-neuron fully-connected layer (*i.e.* the output layer) were initialised by the uniform random distribution as per Glorot et al⁴⁴. The standard *binary cross-entropy* loss function was used for training.

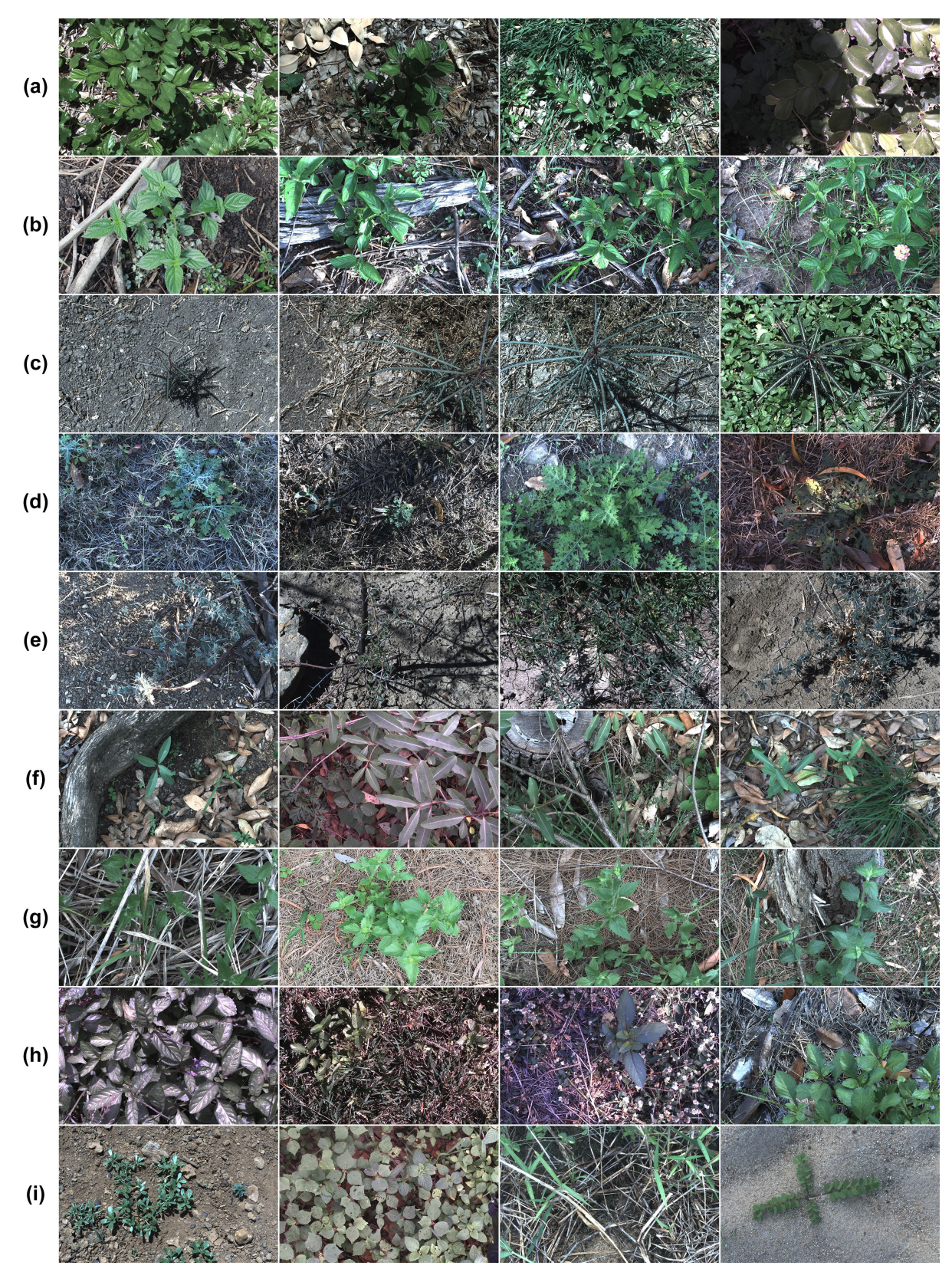


Figure 3. Sample images from each class of the *DeepWeeds* dataset, namely: (a) Chinee apple, (b) Lantana, (c) Parkinsonia, (d) Parthenium, (e) Prickly acacia, (f) Rubber vine, (g) Siam weed, (h) Snake weed and (i) Negatives.

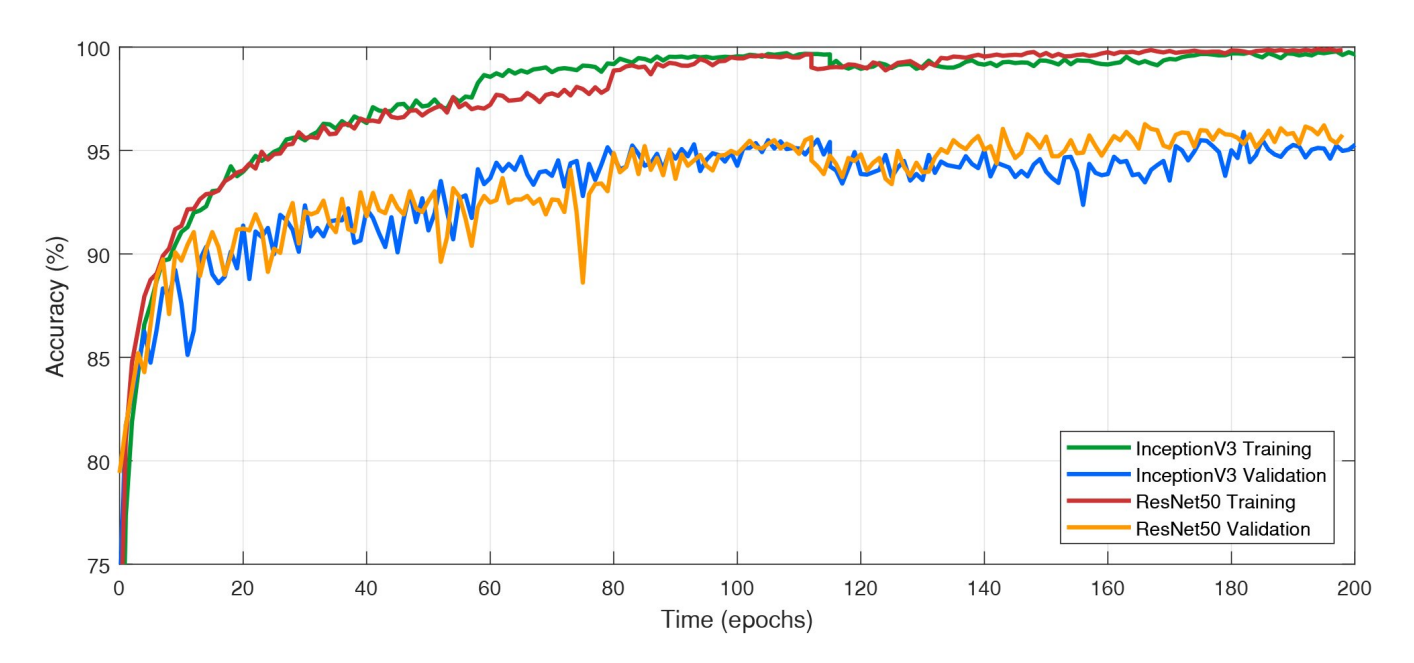


Figure 4. Visualisation of the learning process where the training and validation accuracy for Inception-v3 and ResNet-50 improve after successive epochs; beginning to plateau after 100 epochs and resting at average accuracies above 90%.

To overcome the highly variable nature of the target weed detection application, a series of augmentations were performed on both the training and validation image subsets to account for variations in rotation, scale, colour, illumination and perspective. Image augmentation was performed using the Open Source Computer Vision Library (OpenCV) and its Python wrapper. All images were first resized to 256×256 pixels in size and randomly augmented for each epoch of training, *i.e.* one pass through all available training and validation images. Each image was also randomly rotated in the range of [-360, +360] degrees. Then, each image was randomly scaled both vertically and horizontally in the range of [0.5, 1]. Each colour channel was randomly shifted within the range of ± 25 (*i.e.* approximately $\pm 10\%$ of the maximum available 8-bit colour encoding range [0,255]). To account for illumination invariance, pixel intensity was randomly shifted within the [-25, +25] range, shifting all colour channels uniformly. In addition, pixel intensity was randomly scaled within the [0.75, 1.25] range. Random perspective transformations were applied to each image to simulate a large variation of viewing distances and angles. Finally, the images were flipped horizontally with a 50% probability and then cropped to retain the 224×224 pixels required for each architecture's input layer. With all nine classes of the *DeepWeeds* dataset, the ResNet-50 and Inception-v3 models contained approximately 23.5 million and 21.8 million trainable weights, respectively. Without this extensive augmentation, both CNN networks drastically overfitted the available images by memorising the training subsets.

The Keras implementation of Adam⁴⁵, a first-order gradient-based method for stochastic optimisation, was used for the training of both models. The initial learning-rate (lr) was set to $lr = 1 \times 10^{-4}$. It was then successively halved every time the *validation loss* did not decrease after 16 epochs. Note that the validation loss refers to the classification error computed on the validation subset of images. The training was performed in batches of 32 images, and aborted if the validation loss did not decrease after 32 epochs. While training, the model with the smallest running validation loss was continuously saved, in order to re-start the training after an abortion. In such cases, training was repeated once with the initial learning rate $lr = 0.5 \times 10^{-4}$.

Figure 4 illustrates the learning process for both the Inception-v3 and ResNet-50 models on the *DeepWeeds* training and validation subsets. It can be seen that both methods plateaued in accuracy after roughly 100 epochs. The training was observed to have been aborted and re-started for Inception-v3 and ResNet-50 after 115 and 112 epochs, respectively. The models then continued to slightly improve in accuracy through to 200 epochs. It took approximately 5-6 hours to train one model on an Nvidia GTX 1080Ti GPU, where ResNet-50 and Inception-v3 consumed comparable training times.

Results

The DeepWeeds Dataset

From June 2017 to March 2018, images were collected from sites across northern Australia using the *WeedLogger* in-field instrument. The result is *DeepWeeds*, a large multiclass dataset comprising 17,509 images of eight different weed species and various off-target (or negative) plant life native to Australia.

Table 1.	The distribution	of DeenWeeds	images by weed	species and location.
----------	------------------	--------------	----------------	-----------------------

		Locations								
		Black	Charters	Cluden	Douglas	Hervey	Kelso	McKinlay	Paluma	Total
		River	Towers	Ciuden	Douglas	Range	Keiso	meninay	Ташта	Total
	Chinee apple	0	0	0	718	340	20	0	47	1125
	Lantana	0	0	0	9	0	0	0	1055	1064
	Parkinsonia	0	0	1031	0	0	0	0	0	1031
spa	Parthenium	0	246	0	0	0	776	0	0	1022
	Prickly acacia	0	0	132	1	0	0	929	0	1062
Weeds	Rubber vine	0	188	1	815	0	5	0	0	1009
	Siam weed	1072	0	0	0	0	0	0	2	1074
	Snake weed	10	0	0	928	1	34	0	43	1016
	Negatives	1200	605	1234	2606	471	893	943	1154	9106
	Total	2282	1039	2398	5077	812	1728	1872	2301	17509

Table 1 shows the quantitative distribution of images, sorted by weed species and location. Over 1,000 images were collected of each weed species, totaling over 8,000 images of positive species classes. Images of neighbouring flora and backgrounds that did not contain the weed species of interest were collated into a single "negative" class. To balance any scene bias, an even split of positive and negative samples were collected from each location. This balance can be observed in Figure 5 which maps the geographical distribution of the images.

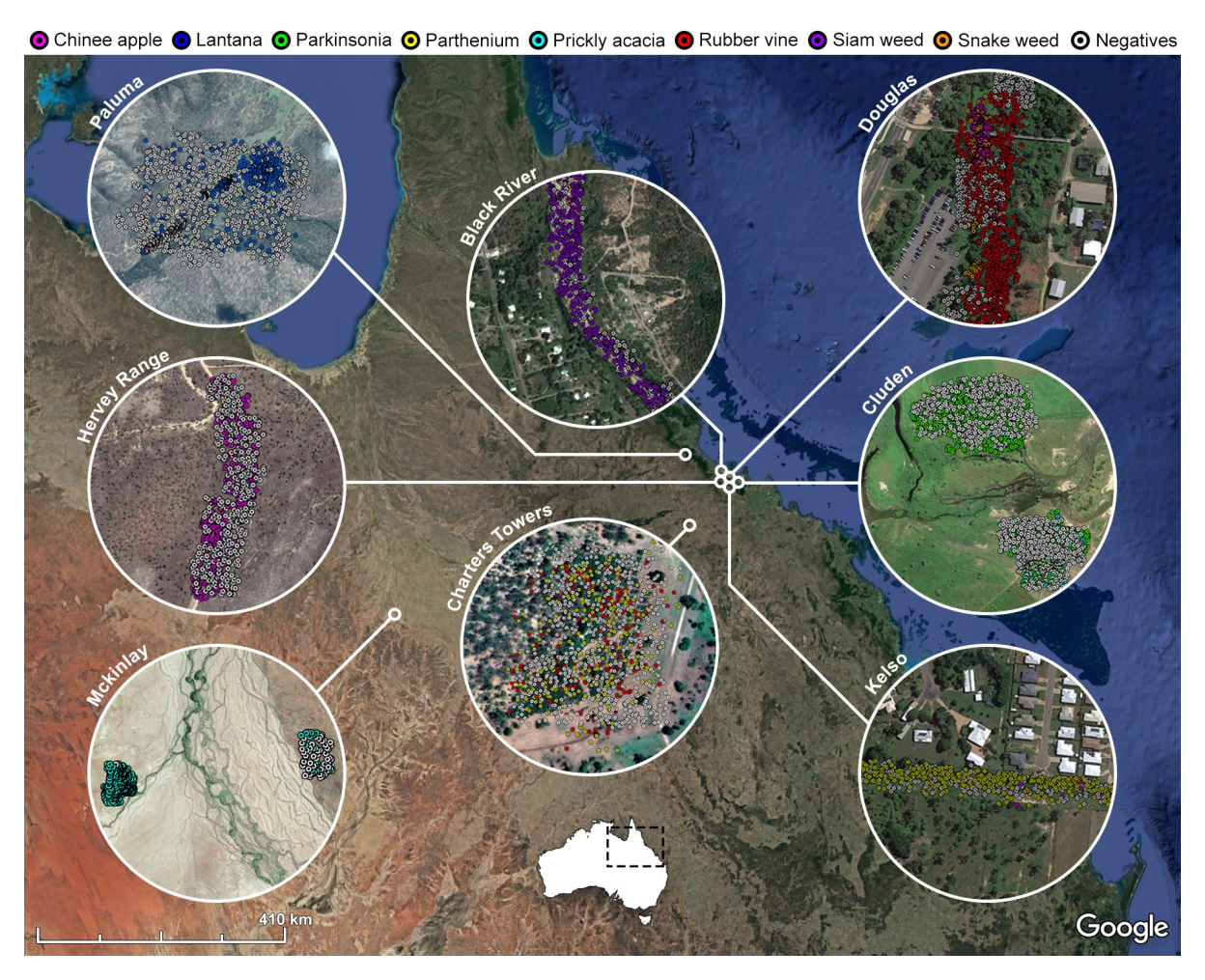


Figure 5. The geographical distribution of *DeepWeeds* images collected throughout northern Australia (Data SIO, NOAA, U.S. Navy, NGA, GEBCO; Image © 2018 Landsat / Copernicus; Image © 2018 DigitalGlobe; Image © 2018 CNES / Airbus).

The breadth of the dataset is also apparent from Figure 5, which spans several collection sites across northern Australia. Each collection site was identified to contain large infestations of specific target species, including: siam weed from *Black River* (19°13′44″ S, 146°37′45″ E), rubber vine from *Charters Towers* (20°04′44″ S, 146°10′55″ E), parkinsonia from *Cluden* (19°19′02″ S, 146°51′02″ E), snake weed from *Douglas* (19°19′29″ S, 146°45′44″ E), chinee apple from *Hervey Range* (19°19′35″ S, 146°38′50″ E), parthenium from *Kelso* (19°22′38″ S, 146°43′05″ E), prickly acacia from *Mckinlay* (21°20′21″ S, 141°31′27″ E) and lantana from *Paluma* (18°57′23″ S, 146°02′17″ E).

Deep Learning Performance

The *DeepWeeds* dataset was classified with the ResNet-50 and Inception-v3 CNN models to establish a baseline level of performance for future comparison. Results are tabulated below. Table 2 documents the mean and standard deviation classification accuracy across five separate trials with uniquely randomised training, validation and testing subsets for the ResNet-50 and Inception-v3 CNN models. Table 3 provides the average within-class confusion matrix across the same five trials for ResNet-50, which was found to perform slightly better than Inception-v3.

Table 2 illustrates that ResNet-50 and Inception-v3 achieved an average classification accuracy of 90.5% and 87.9%, respectively. This is a very strong baseline result. The slightly better performance of the ResNet-50 model may be attributed to its slightly higher complexity, constituting 23.5 million trainable weights, as opposed to 21.8 million for Inception-v3. This added complexity allows for a broader optimisation space within which the ResNet-50 model can learn. In all cases, the training accuracy exceeds the validation and testing accuracy by only a small amount, consequently showing no signs of underfitting or overfitting to the training data. The comparable performance on unseen images from the test subset to images from the validation subset shows that the models generalise well to an independent dataset.

Performance can be seen to vary from species to species for both models. Strongest performance was achieved on Chinee apple at 96.3%, Parkinsonia at 98.6%, Rubber vine at 98.8% and Siam weed at 95.7%. Performance was also solid for Lantana at 87.9%, Parthenium at 87.2% and Snake Weed 86.8%. The weed species causing the lowest classification performance was Prickly acacia, which was correctly detected at a rate of 78.8% by the Inception-v3 model. We suspect the relatively poor performance on Prickly acacia may be due to the weed having less unique visible features to train on.

Table 2. The mean and standard deviation classification accuracy across five randomised trials using ResNet-50 and Inception-v3 to classify each species of the *DeepWeeds* dataset during training, validation and testing.

Weeds	CNN	Training	Validation	Testing
Chinee apple	Inception-v3	0.985 ± 0.019	0.944 ± 0.033	0.947 ± 0.035
	ResNet-50	0.982 ± 0.015	0.953 ± 0.031	0.963 ± 0.010
Lantana	Inception-v3	0.917 ± 0.014	0.847 ± 0.026	0.827 ± 0.031
	ResNet-50	0.935 ± 0.025	0.877 ± 0.055	0.879 ± 0.018
Parkinsonia	Inception-v3	0.951 ± 0.028	0.934 ± 0.032	0.935 ± 0.036
	ResNet-50	0.991 \pm 0.007	0.978 ± 0.007	0.986 ± 0.012
Parthenium	Inception-v3	0.820 ± 0.098	0.783 ± 0.117	0.795 ± 0.085
	ResNet-50	0.902 ± 0.045	0.880 ± 0.043	0.872 ± 0.045
Prickly acacia	Inception-v3	0.843 ± 0.086	0.779 ± 0.061	0.788 ± 0.085
	ResNet-50	0.827 ± 0.077	0.758 ± 0.074	0.785 ± 0.061
Rubber vine	Inception-v3	0.994 ± 0.004	0.971 ± 0.018	0.972 ± 0.019
	ResNet-50	0.996 ± 0.004	0.990 ± 0.006	0.988 \pm 0.011
Siam weed	Inception-v3	0.956 ± 0.027	0.898 ± 0.050	0.887 ± 0.046
	ResNet-50	0.984 ± 0.012	0.957 ± 0.025	0.957 ± 0.021
Snake weed	Inception-v3	0.918 ± 0.037	0.838 ± 0.055	0.831 ± 0.051
	ResNet-50	0.929 ± 0.037	0.857 ± 0.027	0.868 \pm 0.051
Negatives	Inception-v3	0.963 ± 0.013	0.939 ± 0.014	0.931 ± 0.014
	ResNet-50	0.888 ± 0.020	0.856 ± 0.016	0.843 ± 0.013
Average	Inception-v3	0.928 ± 0.074	0.881 ± 0.087	0.879 ± 0.084
	ResNet-50	0.937 ± 0.064	0.901 ± 0.080	0.905 ± 0.075

Weeds	Chinee	Lantana	Parkinsonia	Parthenium	Prickly	Rubber	Siam	Snake	Negatives
	apple				acacia	vine	weed	weed	
Chinee apple	96.19	3.6	0.1	0.6	0.5	0.3	0.1	8.3	3.4
Lantana	0.2	87.76	0	0	0.4	0	0.5	0.4	1.6
Parkinsonia	0	0	98.61	0.7	8.2	0	0	0	1.4
Parthenium	0	0	0.3	86.88	2.3	0.1	0	0	1.1
Prickly acacia	0	0	0.1	0.7	77.88	0	0	0	0.8
Rubber vine	0.3	1.0	0	0.4	0.2	98.74	0.5	1.1	2.8
Siam weed	0	0.8	0.1	0.2	0	0	95.51	0	1.6
Snake weed	1.5	3.3	0	0.4	0.6	0	0.2	86.45	3.1
Negatives	1.8	3.5	0.8	10.1	10.0	0.8	3.2	3.8	84.31

Table 3. The confusion matrix (%) achieved by the ResNet-50 model on the five randomised test subsets.

Table 3 shows the confusion matrix resulting from averaging the ResNet-50 model's performance across the test subsets. The model confuses 8.3% of chinee apple images with snake weed. Reviewing these particular samples shows that under certain lighting conditions the leaf material of chinee apple looks strikingly similar to that of snake weed. This is illustrated in Figure 6. Similarly, the ResNet-50 model incorrectly classifies 8.2% of parkinsonia images as prickly acacia. Figure 6 shows one sample misclassification. It should be noted that parkinsonia and prickly acacia are from the same genus, and are commonly both known as prickle bush species. In addition to their similar shape and size, they both produce thorns, yellow flowers and bean-like seed pods. This likeness is the reason for these false positives in our model.



Figure 6. Example images highlighting common confusions between classes of weed species. Specifically, (a) correctly classified snake weed, (b) chinee apple falsely classified as snake weed, (c) correctly classified prickly acacia, and (d) parkinsonia falsely classified as prickly acacia.

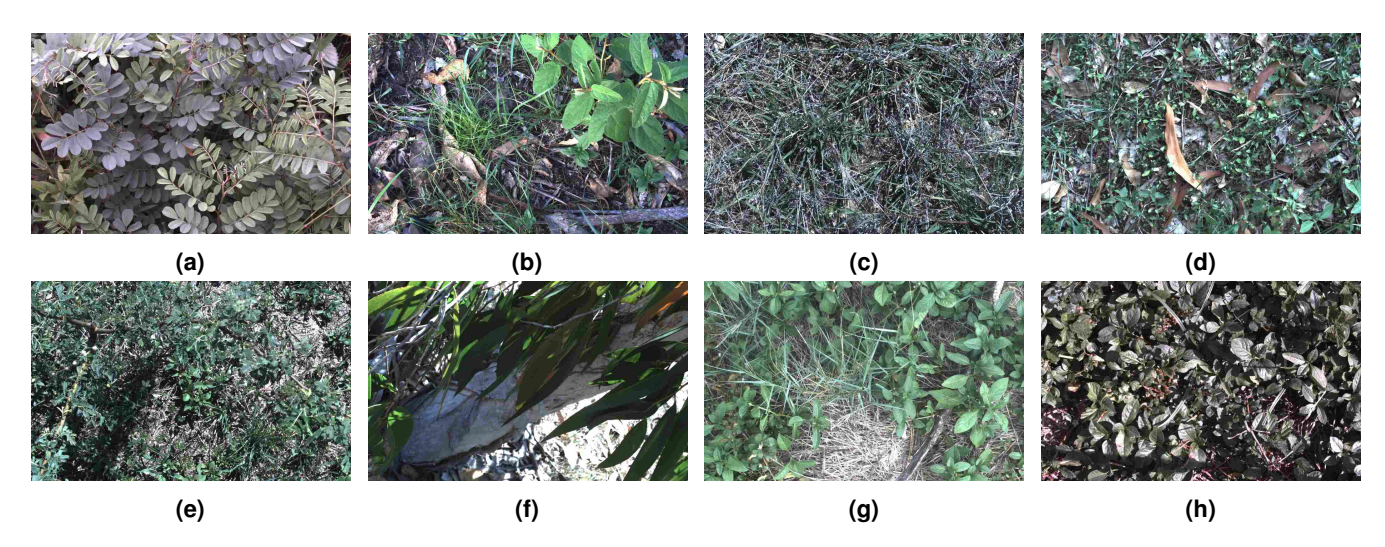


Figure 7. Example false positive images where, due to strong visual similarity, images from the negative class were falsely classified as (a) Chinee apple, (b) Lantana, (c) Parkinsonia, (d) Parthenium, (e) Prickly acacia, (f) Rubber vine, (g) Siam weed and (h) Snake weed.

While these minor confusions are indeed limitations of the learning model, we should highlight that chinee apple, snake weed, parkinsonia and prickly acacia are all weeds that need to be controlled. So confusing one for the other when eradicating them all is inconsequential. Of more concern are false positives where established native plant life is incorrectly classified as weeds. This may cause harm to the native ecosystem, as well as waste herbicide on non-target plant life. The confusion matrix of Table 3 shows that we have incorrectly classified 10.1% of negatives as parthenium and another 10.0% of negatives as prickly acacia. To understand why this has happened, Figure 7 shows examples of where a negative has been misclassified as each of the eight target weed species. In every case, a native plant has been identified that closely resembles each species. This shows that the immense variation in plant life that makes up the negative class does introduce unavoidable false positives. However, their occurrence is a rarity and the robotic control method will only generally be applied in areas with dense infestations of the target weed, where native plant life is sparse.

Discussion

In summary, this work introduces the first, large, multiclass weed species image dataset collected entirely in situ from Australian rangelands. *DeepWeeds* contains eight weed species of national significance to Australia, and spans eight geographic locations from northern Australia. We also present strong baseline performance using the Inception-v3 and ResNet-50 CNN models, that achieve an average classification performance of 87.9% and 90.5%, respectively. This is a strong result and further proves the power of deep learning for highly variable image datasets.

We anticipate that the dataset and our classification results will inspire further research into the detection of rangeland weeds under realistic conditions. Future work in this area includes: improving the accuracy and robustness of classifying the *DeepWeeds* dataset, field implementation of our learning models as the detection system for a prototype weed control robot and investigating the use of NIR spectroscopy and hyperspectral imaging for weed species detection. The great lengths taken to collect a dataset including the real life complexity of the rangeland environment should allow for strong in-field performance.

Data Availability

The *DeepWeeds* dataset, generated and analysed during the current study, is publicly available through the corresponding author's QRIScloud Nextcloud file share repository: https://nextcloud.griscloud.org.au/index.php/s/acal4xJ6n5O2mjT.

References

- **1.** Gonzalez-de Santos, P. *et al.* Fleets of robots for environmentally-safe pest control in agriculture. *Precis. Agric.* **18**, 574–614 (2017).
- **2.** Fernández-Quintanilla, C. *et al.* Is the current state of the art of weed monitoring suitable for site-specific weed management in arable crops? *Weed Res.* **58**, 259–272 (2018).
- 3. Commonwealth of Australia. Agricultural competitiveness white paper (2015). ISBN: 978-1-925237-73-3.
- **4.** Slaughter, D. C., Giles, D. K. & Downey, D. Autonomous robotic weed control systems: A review. *Comput. Electron. Agric.* **61**, 63–78 (2008).
- 5. Shaner, D. L. & Beckie, H. J. The future for weed control and technology. *Pest Manag. Sci.* 70, 1329–1339 (2014).
- **6.** Bakhshipour, A. & Jafari, A. Evaluation of support vector machine and artificial neural networks in weed detection using shape features. *Comput. Electron. Agric.* **145**, 153 160 (2018).
- 7. dos Santos Ferreira, A., Freitas, D. M., da Silva, G. G., Pistori, H. & Folhes, M. T. Weed detection in soybean crops using ConvNets. *Comput. Electron. Agric.* 143, 314 324 (2017).
- **8.** Dyrmann, M., Jørgensen, R. N. & Midtiby, H. S. RoboWeedSupport Detection of weed locations in leaf occluded cereal crops using a fully convolutional neural network. *Adv. Animal Biosci.* **8**, 842–847 (2017).
- Wu, S. G. et al. A leaf recognition algorithm for plant classification using probabilistic neural network. In Proceedings of the 2007 IEEE International Symposium on Signal Processing and Information Technology (ISSPIT), 11–16 (Cairo, Egypt, 2007).
- **10.** Kumar, N. *et al.* Leafsnap: A computer vision system for automatic plant species identification. In *Proceedings of the 2012 European Conference on Computer Vision (ECCV)*, 502–516 (Berlin, Heidelberg, 2012).
- 11. Hall, D., McCool, C., Dayoub, F., Sunderhauf, N. & Upcroft, B. Evaluation of features for leaf classification in challenging conditions. In *Proceedings of the 2015 IEEE Winter Conference on Applications of Computer Vision (WACV)*, 797–804 (Hawaii, USA, 2015).

- 12. Kalyoncu, C. & Önsen Toygar. Geometric leaf classification. Comput. Vis. Image Underst. 133, 102 109 (2015).
- **13.** Lee, S. H., Chan, C. S., Mayo, S. J. & Remagnino, P. How deep learning extracts and learns leaf features for plant classification. *Pattern Recognit.* **71**, 1–13 (2017).
- **14.** Lee, S. H., Chan, C. S., Wilkin, P. & Remagnino, P. Deep-plant: Plant identification with convolutional neural networks. In *Proceedings of the 2015 IEEE International Conference on Image Processing (ICIP)*, 452–456 (Québec City, Canada, 2015).
- **15.** Carranza-Rojas, J., Goeau, H., Bonnet, P., Mata-Montero, E. & Joly, A. Going deeper in the automated identification of herbarium specimens. *BMC Evol. Biol.* **17**, 181 (2017).
- **16.** Shirzadifar, A., Bajwa, S., Mireei, S. A., Howatt, K. & Nowatzki, J. Weed species discrimination based on SIMCA analysis of plant canopy spectral data. *Biosyst. Eng.* **171**, 143 154 (2018).
- **17.** Li, L., Wei, X., Mao, H. & Wu, S. Design and application of spectrum sensor for weed detection used in winter rape field. *Transactions Chin. Soc. Agric. Eng.* **33**, 127–133 (2017).
- **18.** Louargant, M. *et al.* Unsupervised classification algorithm for early weed detection in row-crops by combining spatial and spectral information. *Remote. Sens.* **10**, 761 (2018).
- **19.** Lin, F., Zhang, D., Huang, Y., Wang, X. & Chen, X. Detection of corn and weed species by the combination of spectral, shape and textural features. *Sustainability* **9**, 1335 (2017).
- **20.** Mahesh, S., Jayas, D., Paliwal, J. & White, N. Hyperspectral imaging to classify and monitor quality of agricultural materials. *J. Stored Prod. Res.* **61**, 17 26 (2015).
- **21.** Olsen, A., Han, S., Calvert, B., Ridd, P. & Kenny, O. In situ leaf classification using histograms of oriented gradients. In *Proceedings of the 2015 International Conference on Digital Image Computing: Techniques and Applications (DICTA)*, 441–448 (Adelaide, Australia, 2015).
- **22.** Wäldchen, J. & Mäder, P. Plant species identification using computer vision techniques: A systematic literature review. *Arch. Comput. Methods Eng.* **25**, 507–543 (2017).
- 23. LeCun, Y., Bengio, Y. & Hinton, G. Deep learning. *Nature* 521, 436–444 (2015).
- **24.** Krizhevsky, A., Sutskever, I. & Hinton, G. E. ImageNet classification with deep convolutional neural networks. In *Proceedings of the 25th International Conference on Neural Information Processing Systems (NIPS)*, vol. 1, 1097–1105 (Lake Tahoe, USA, 2012).
- **25.** Joly, A. *et al.* LifeCLEF 2015: Multimedia Life Species Identification Challenges. In *Proceedings of the 2015 International Conference of the Cross-Language Evaluation Forum for European Languages (CLEF)*, vol. 1391, 462–483 (Toulouse, France, 2015).
- **26.** Joly, A. et al. LifeCLEF 2016: Multimedia Life Species Identification Challenges. In *Proceedings of the 2016 International Conference of the Cross-Language Evaluation Forum for European Languages (CLEF)*, 286–310 (Évora, Portugal, 2016).
- 27. Joly, A. et al. LifeCLEF 2017 Lab Overview: Multimedia Species Identification Challenges. In *Proceedings of the 2017 International Conference of the Cross-Language Evaluation Forum for European Languages (CLEF)*, 255–274 (Dublin, Ireland, 2017).
- **28.** Pérez-Ortiz, M. *et al.* A semi-supervised system for weed mapping in sunflower crops using unmanned aerial vehicles and a crop row detection method. *Appl. Soft Comput.* **37**, 533 544 (2015).
- **29.** Tang, J.-L., Chen, X.-Q., Miao, R.-H. & Wang, D. Weed detection using image processing under different illumination for site-specific areas spraying. *Comput. Electron. Agric.* **122**, 103 111 (2016).
- **30.** Barrero, O., Rojas, D., Gonzalez, C. & Perdomo, S. Weed detection in rice fields using aerial images and neural networks. In *Proceedings of the 2016 XXI Symposium on Signal Processing, Images and Artificial Vision (STSIVA)*, 1–4 (Bucaramanga, Colombia, 2016).
- **31.** Australian Weeds Committee. Weeds of national significance 2012 (Department of Agriculture, Fisheries and Forestry, Canberra, ACT, Australia, 2012). ISBN: 978 0 9803249 3 8.
- 32. Moeslund, T. B. Introduction to Video and Image Processing (Springer-Verlag London, 2012).
- **33.** Goodfellow, I., Bengio, Y. & Courville, A. *Deep Learning* (MIT Press, 2016).
- **34.** Chollet, F. et al. Keras. https://keras.io (2015).
- 35. Abadi, M. et al. TensorFlow: Large-scale machine learning on heterogeneous systems. https://www.tensorflow.org (2015).

- **36.** Szegedy, C., Vanhoucke, V., Ioffe, S., Shlens, J. & Wojna, Z. Rethinking the inception architecture for computer vision. In *Proceedings of the 2016 IEEE Conference on Computer Vision and Pattern Recognition (CVPR)*, 2818–2826 (Las Vegas, USA, 2016).
- **37.** Szegedy, C. *et al.* Going deeper with convolutions. In *Proceedings of the 2015 IEEE Conference on Computer Vision and Pattern Recognition (CVPR)*, 1–9 (Boston, USA, 2015).
- 38. Russakovsky, O. et al. ImageNet large scale visual recognition challenge. Int. J. Comput. Vis. 115, 211–252 (2015).
- **39.** He, K., Zhang, X., Ren, S. & Sun, J. Deep residual learning for image recognition. In *Proceedings of the 2016 IEEE Conference on Computer Vision and Pattern Recognition (CVPR)*, 770–778 (Las Vegas, USA, 2016).
- **40.** Simonyan, K. & Zisserman, A. Very deep convolutional networks for large-scale image recognition. In *Proceedings of the 2015 International Conference on Learning Representations (ICLR)* (San Diego, USA, 2015).
- **41.** Zeng, X. *et al.* Crafting GBD-Net for object detection. *IEEE Transactions on Pattern Analysis Mach. Intell.* **40**, 2109–2123 (2016).
- 42. Hu, J., Shen, L. & Sun, G. Squeeze-and-excitation networks. arXiv preprint arXiv: 1709.01507 (2017).
- **43.** Oquab, M., Bottou, L., Laptev, I. & Sivic, J. Learning and transferring mid-level image representations using convolutional neural networks. In *Proceedings of the 2014 IEEE Conference on Computer Vision and Pattern Recognition (CVPR)*, 1717–1724 (Boston, USA, 2014).
- **44.** Glorot, X. & Bengio, Y. Understanding the difficulty of training deep feedforward neural networks. In *Proceedings of the 13th International Conference on Artificial Intelligence and Statistics (AISTATS)*, vol. 9, 249–256 (Sardinia, Italy, 2010).
- **45.** Kingma, D. P. & Ba, J. Adam: A method for stochastic optimization. In *Proceedings of the 3rd International Conference on Learning Representations (ICLR)* (San Diego, USA, 2015).

Acknowledgments

This work is funded by the Australian Government Department of Agriculture and Water Resources Control Tools and Technologies for Established Pest Animals and Weeds Programme (Grant No. 4-53KULEI).

Author contributions statement

A.O. and D.A.K. wrote the manuscript. A.O., D.A.K. and B.P. conceived the experiments. A.O., P.R., J.C.W., J.J., W.B. and B.G. collected the dataset. P.R., R.D.W., B.P., A.O., O.K., J.W., M.R.A. and B.C. conceived the project. B.P., P.R., R.D.W., M.R.A., O.K. and B.C. reviewed the manuscript.

Additional information

Competing Interests: The authors declare no competing interests.